Gas-Phase Nitrosation of Ethylene and Related Events in the C₂H₄NO⁺ Landscape

Pascal Gerbaux,[†] Noemie Dechamps,[†] Robert Flammang,[†] Pham Cam Nam,[‡] Minh Tho Nguyen,[§] Fayçal Djazi,[||] Florence Berruyer,[⊥] and Guy Bouchoux*,[#]

Laboratoire de Chimie Organique, Université de Mons-Hainaut, Avenue Maistriau 19, B-7000 Mons, Belgique, Faculty of Chemical Engineering, University of Danang, Danang, Vietnam, Department of Chemistry, and Mathematical Modelling and Computational Science Centre (LMCC), University of Leuven, B-3001 Leuven, Belgium, Laboratoire de Physicochimie des Surfaces et Interfaces, Département des Sciences Fondamentales, Université de Skikda, BP 26, 21000 Skikda, Algérie, Laboratoire de Chimie Physique, Groupe de Chimie Théorique, UMR CNRS 8000, Bâtiment 490, Université Paris-Sud, F-91405 Orsay Cedex, France, Laboratoire des Mécanismes Réactionnels, UMR CNRS 7651, and Département de Chimie, Ecole Polytechnique, F- 91128 Palaiseau Cedex, France

The C₂H₄NO⁺ system has been examined by means of quantum chemical calculations using the G2 and G3B3 approaches and tandem mass spectrometry experiments. Theoretical investigation of the C₂H₄NO⁺ potential-energy surface includes 19 stable C₂H₄NO⁺ structures and a large set of their possible interconnections. These computations provide insights for the understanding of the (i) addition of the nitrosonium cation NO⁺ to the ethylene molecule, (ii) skeletal rearrangements evidenced in previous experimental studies on comparable systems, and (iii) experimental identification of new C₂H₄NO⁺ structures. It is predicted from computation that gas-phase nitrosation of ethylene may produce C₂H₄•NO⁺ adducts, the most stable structure of which is a π-complex, **1**, stabilized by ca. 65 kJ/mol with respect to its separated components. This complex was produced in the gas phase by a transnitrosation process involving as reactant a complex between water and NO⁺ (H₂O.NO⁺) and the ethylene molecule and fully characterized by collisional experiments. Among the other C₂H₄NO⁺ structures predicted by theory to be protected against dissociation or isomerization by significant energy barriers, five were also experimentally identified. These finding include structures CH₃CHNO⁺ (**5**), CH₃CNOH⁺ (**8**), CH₃NHCO⁺ (**18**), CH₃NCOH⁺ (**19**), and an ion/neutral complex CH₂O•••HCNH⁺ (**12**).

Introduction

Nitric oxide chemistry plays a crucial role in many areas, from atmospheric events to physiological regulation. This diatomic radical was named *The Molecule of the Year 1992* by *Science* magazine for its many surprising beneficial roles, and its ubiquitous role in organic and inorganic chemistry as well as in biochemistry has been comprehensively covered.[1] However, a full understanding of the reactivity of NO cannot be separated from that of its ionized counterpart, the nitrosonium cation NO⁺. Accordingly, the ionization energy of NO of 9.264 eV[2] is close to that of a large range of organic, inorganic, or bioorganic substrates, and thus, charge-transfer processes are expected to play a significant role in the observed reactivity. As a consequence, one of the peculiar processes in NO chemistry is formation of nitrosonium complexes, particularly with π-electron systems. Indeed, numerous examples of complexes involving NO⁺ and various substrates have been described in both the condensed phase and the gas phase.[3] In solution, long-lived olefinic π complexes were proposed as intermediates during reactions of alkene with nitrosyl halides or nitrosonium salts, generally leading to dimerization or isomerization into the more stable oxime tautomers.[3a] Nitrosation of dienes and subsequent transformation into substituted aldehydes has been also demonstrated to be initiated by formation of a π complex.[3b] The ability of NO⁺ to produce stable π complexes with aromatic compounds in the gas phase has long been recognized.[4–10] Experimental complexation energies of such species are generally considerable, in the range of 100−200 kJ/mol.[5,6] On the contrary, fewer examples of reactions of NO⁺ with olefins in the gas phase have been reported.[11–14] Although formation of olefin/NO⁺ association products is generally observed, hydride-ion abstraction, charge exchange, and even more complex reactions involving NO⁺ insertion and significant unimolecular rearrangements are also noteworthy, particularly with 1-alkenes. For example, quantitative elimination of lower alkenes is observed from the olefin/NO⁺ adduct involving 1-alkene (from 1-hexene to 1-docosene),[11a,14] whereas C₄H₇N⁺ ions are produced with 1-butene[11a,13] and CH₄N⁺ ions are formed with 1-pentene, 1-hexene, 1-heptene, and 1-octene.[12,14]

Surprisingly, experimental information of the prototypical ethylene + NO⁺ system is poorly documented. Hunt and Harvey[11a] considered that in their experimental conditions ethylene was nonreactive. More recently, McEwan et al.[15] showed using a flow tube apparatus that the direct condensation reaction occurs but is extremely slow since it proceeds at only 0.1% of the collision rate. From a theoretical point of view, the ethylene + NO⁺ system was computationally examined more than 20 years ago with geometry optimization performed at the Hartree−Fock level with the minimal basis set HF/STO-3G.[16] Obviously, this modest theoretical level is probably not fully appropriate for the description of π complexes, and an updated

* To whom correspondence should be addressed. E-mail: bouchoux@ dcmr.polytechnique.fr.
† Université de Mons-Hainaut.
‡ University of Danang.
§ University of Leuven.
|| Université de Skikda.
⊥ Université Paris-Sud.
Ecole Polytechnique.

Gas-Phase Nitrosation of Ethylene

J. Phys. Chem. A, Vol. 112, No. 24, 2008 **5419**

investigation using more accurate quantum chemical methods is necessary. Moreover, a theoretical exploration of the potential-energy surface in the vicinity of the ethylene + NO^+ π complex is lacking. Such information is obviously of interest in describing the olefinic nitrosation process and, more generally, the isomerization/dissociation reactions revealed by experiments on higher homologue systems. In this context, we set out to investigate both experimentally and computationally a large part of the $C_2H_4NO^+$ system, including the ethylene + NO^+ entry. We thus mapped out portions of the $C_2H_4NO^+$ potential-energy surface involving ethylene + NO^+ complexes and several of their potentially important isomeric forms. The calculations were conducted at the MP2/6-31G(d,p) level of theory, associated with G2 and G3B3 calculations on the various local minima and transition structures. A number of candidates evidenced by quantum chemical computations were produced and examined by mass spectrometric techniques using collisional activation experiments. The first successful experimental characterization of stable ethylene + NO^+ complexes is reported together with five other $C_2H_4NO^+$ structures.

Experimental and Computational Section

The spectra were recorded on a large-scale tandem mass spectrometer (Waters AutoSpec 6F, Manchester) combining six sectors of $c_1E_1B_1c_2E_2c_3c_4E_3B_2c_5E_4$ geometry (E stands for electric sector, B for magnetic sector, and c for collision cell).[17] General conditions were as follows: 8 kV accelerating voltage, 200 μA trap current in the electron ionization mode, EI, and 1 mA in the chemical ionization mode, CI, 70 eV ionizing electron energy, and 200 °C ion source temperature. The samples were introduced with a direct insertion probe or via a heated (180 °C) septum inlet.

Installation of an rf-only quadrupole collision cell (Q_{cell}) inside the instrument between E_2 and E_3 was also reported elsewhere.[18] This modification allows the study of ion/molecule reactions and collisional activation of decelerated ions. Briefly, the experiments utilizing the Q_{cell} consist of selection of a beam of fast ions (8 keV) with the three first sectors ($E_1B_1E_2$) and deceleration of these ions to approximately 5 eV (to maximize ion–molecule reactions) or 20–30 eV (to maximize collision-induced dissociations). The interaction between the ions and the reagent gas (the pressure of the gas is estimated to be about 10^{-3} Torr) is thereafter realized in the Q_{cell}, and after reacceleration at 8 keV, all the ions generated in the quadrupole are separated and mass measured by scanning the field of the second magnet. The high-energy CA spectra of mass-selected ions generated in the Q_{cell} can be recorded by scanning the field of the last electric sector after mass selection by the second magnet and collision in the fifth (c_5) collision cell.

Quantum chemical calculations were carried out using the Gaussian 03 set of programs.[19,20] Geometry optimizations of the stationary points were initially conducted at the second-order perturbation theory (MP2) of molecular orbital theory and the popular hybrid B3LYP functional of density functional theory using the 6-31G(d,p) basis set. Improved calculations have been done using the composite methods G2 and G3B3 for structures corresponding to local minima of the potential-energy surface in order to provide heats of formations within an expected accuracy of ca. ±5−10 kJ/mol.[16] The identity of each transition structure connecting two relevant equilibrium structures was identified by intrinsic reaction coordinate (IRC) calculations.

Results and Discussion

Computational Results. In view of the first objective of this study, investigation of the $C_2H_4NO^+$ system has first been

SCHEME 1
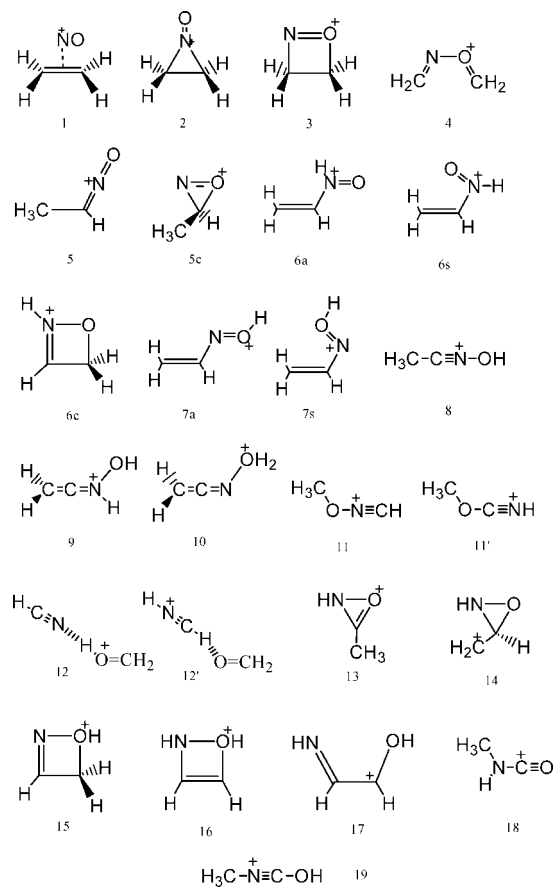
conducted on structures containing both CC and NO linkages. However, as indicated in the Introduction, several structures connected by simple skeletal rearrangement were also investigated. As a consequence, 19 stable structures, denoted from **1** to **19**, were identified (Scheme 1). Their optimized geometries are presented in Figure 1, and their total and relative energies are reported in Table S1 of the Supporting Information. Note that only structures **1**, **2**, **3**, **6**, and **7** were previously located by geometry optimization at the HF/STO-3G level.[16] Total and relative energies of the transition structures located between stable structures **1** and **9** are gathered in Table S2 of the Supporting Information. Note that relative energies calculated at the G3B3 level (or G2 into parentheses) are also reported in Schemes 2–6 and Figures 2–6.

Three stable structures were found to match with a condensation of ethylene and NO^+, namely, ions **1**, **2**, and **3** shown in Scheme 2. Among these three structures, the two latter appear to be only moderately stabilized with respect to their two separated components. Obviously in such cases, the ring strain energy counterbalances the energy gain provided by the covalent bond formation. The most stable structure **1** is characterized by C_s point group symmetry, and C···N distances of 2.5 and 3.1 Å clearly demonstrate the absence of a covalent bond. The electrostatic interaction at the origin of the stability of **1** is mainly due to the Coulombic attraction between the nitrogen atom (net charge = +0.54, Mulliken population analysis at the MP2/6-31G(d,p) level) and the two carbon atoms (net charge = −0.27 on each C, Mulliken population analysis at the MP2/6-31G(d,p) level). The remaining positive charge of complex **1** is shared between the four hydrogen atoms and, to a lesser extent, the oxygen atom. The calculated NO^+ binding energy of this π complex is equal to 65 kJ/mol at 298 K at the G3B3 level. This
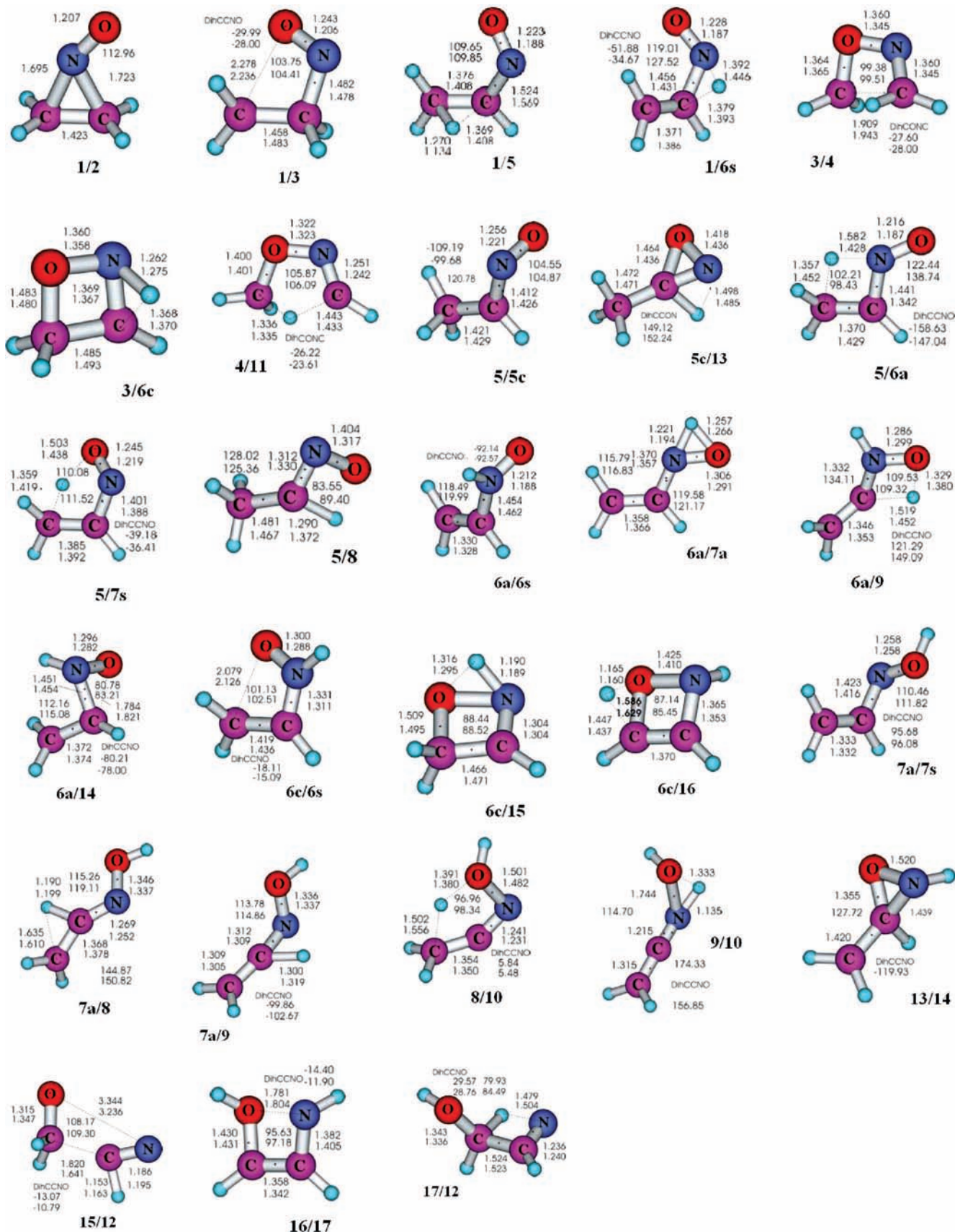
Gas-Phase Nitrosation of Ethylene

J. Phys. Chem. A, Vol. 112, No. 24, 2008 **5421**
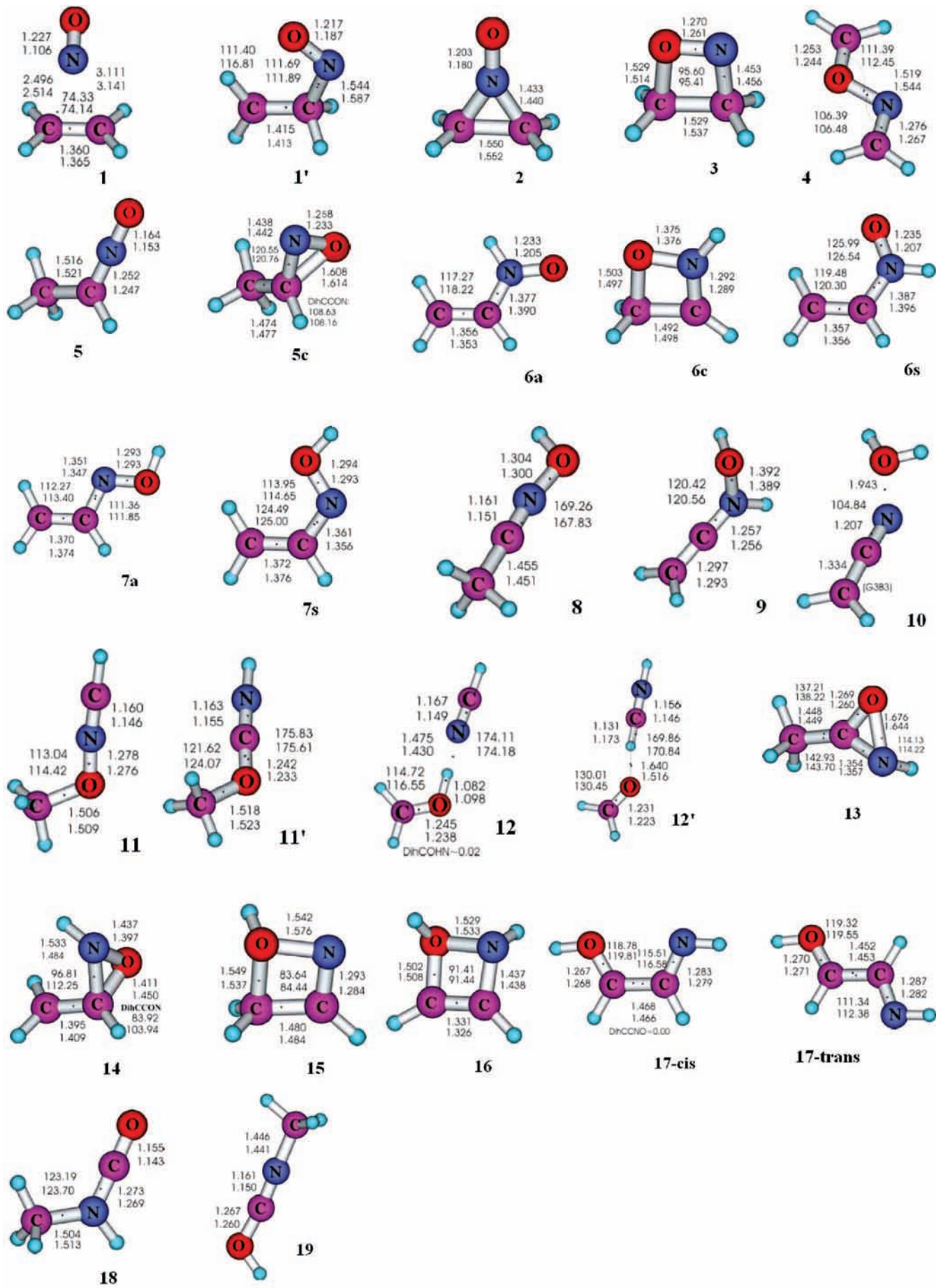
Figure 1. Selected MP2/6-31G(d,p) and B3LYP/6-31G(d,p) geometry parameters of stable structures **1**−**19** and their related transition structures (bond lengths in Ångstroms and bond angles in degrees).

value is significantly lower than the stabilization energy between benzene and NO$^+$ for which a value of 131 kJ/mol has been experimentally determined.[6] Possibilities for isomerization reac-

tions between structures **1**, **2**, and **3** were investigated. During this search we attempted to locate a covalently bonded intermediate CH$_2$CH$_2$NO$^+$ (**1′**). This structure lies in a very

SCHEME 2
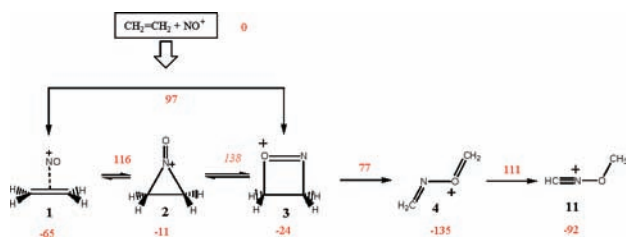
SCHEME 3

SCHEME 4

shallow potential-energy well located 77 kJ/mol above the NO$^+$ + ethylene asymptote at the HF/6-31G(d) level but collap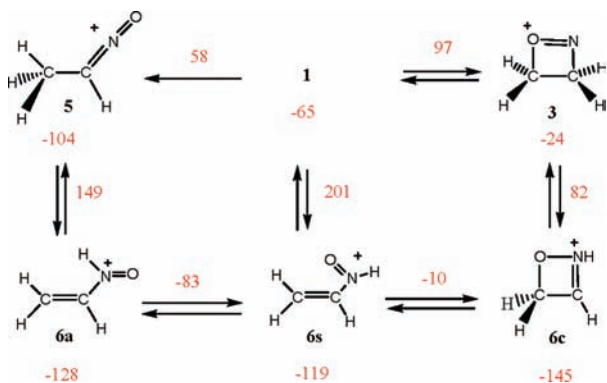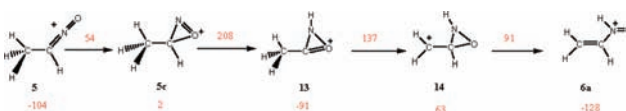ses to **1** at higher levels of theory (Figure 1). Both isomerization routes **1 → 2** and **1 → 3** are associated with transition structures situated 116 and 97 kJ/mol above ethylene + NO$^+$, respectively. It should be noted that for these two processes most of the critical energy content is associated with C–N bond breaking leading to an opened structure looking like **1′**. Trying to locate a transition structure for the direct **2 → 3** isomerization step failed. However, a two-step process involving separate ring opening/ring closure was identified at the HF/6-31G(d) level, the highest energy of which corresponds to the 138 kJ/mol relative energy (MP2/6-31G(d)//HF/6-31G(d), 298 K calculations) given in italics in Scheme 2 and Figure 2. What is evident from these calculated results is that for the three structures **1**, **2**, and **3** dissociation is much easier to achieve than isomerization.

Interestingly, cyclic structure **3** may give rise to an inclusion of the NO moiety into the C=C bond by a simple ring opening (Scheme 2). The open form of **3** corresponds to structure **4**, having a good stability. The conrotatory ring opening of **3** needs a non-negligible critical energy (101 kJ/mol) since the system has to attain a large CC distance value (of 1.91 Å) before recovering the full π resonance developed in **4**. One may note also that only the anti conformation of **4** (Figure 2) has been found to be stable; the syn conformer is in fact the transition structure for the rotation around the N–O bond, which is situated 81 kJ/mol below the CH$_2$=CH$_2$ + NO$^+$ point at the G2 level. It is also noteworthy that **4** may isomerize to CH$_3$ONCH$^+$ ion **11** by a 1,4-hydrogen migration, but the reaction needs a considerable amount of activation energy (~250 kJ/mol). A summary of the 298 K enthalpy diagram associated with Scheme 2 is given in Figure 2.

Evolution of the primary NO$^+$/ethylene adducts toward structures CH$_3$CH=N=O$^+$ (**5**) and CH$_2$=CHNH=O$^+$ (**6**) was

explored (Scheme 3). Two conformations syn and anti, denoted as **6s** and **6a**, were identified for ion **6**. Moreover, a cyclic form **6c** was located and found to be the most stable among the structures **5** and **6**. At the G3B3 level, structures **5**, **6s**, **6a**, and **6c** are more stable than the ethylene/NO$^+$ isolated reactants by 104, 119, 128, and 145 kJ/mol, respectively.

We find that **5** and **6s** can be formed directly by 1,2-H shifts from structure **1**. The corresponding transition structures are situated at 58 and 201 kJ/mol above CH$_2$=CH$_2$ + NO$^+$. Formation of the cyclic ion **6c** may occur either from **3** through a 1,2-hydrogen shift or from cyclization of **6s**. The former reaction **1 → 3 → 6c** is easier to achieve than formation of **6c** from **1** via passage through **6s** since the difference in overall critical energies is 105 kJ/mol.

Structures **5** and **6** may interconvert to each other directly by a 1,3-hydrogen migration between the terminal carbon and nitrogen atoms **5 → 6a**. It emerges from the calculations that the latter process involves a large critical energy (253 kJ/mol), which is however not uncommon for a 1,3-hydrogen migration. The rotational barrier separating the two conformers **6a** and **6s** and cyclization of the syn conformer **6s** to generate structure **6c** are associated with transition-state energies situated 83 and 10 kJ/mol below NO$^+$ + ethylene. Interconversion between these three structures is consequently facile. The 298 K enthalpy diagram associated with Scheme 3 is given in Figure 3. It clearly appears from examination of Figure 3 that structures **5** and the mixture of structures **6a/6s/6c** are separated by energy barriers well above the CH$_2$=CH$_2$ + NO$^+$ products. This means that isomerization of these species into **1** or **3** would lead to dissociation. The second consequence is that ions of structures **5** or **6** possessing not enough internal energy to isomerize may be experimentally characterized.

Starting now from structures **5** and **6**, a second flow of isomerization reactions was investigated. During exploration of the C$_2$H$_4$NO$^+$ potential-energy surface near **5** we found that a cyclic form **5c** presents a reasonable stability. This structure is situated 106 kJ/mol above **5**, and its formation from **5** via transition structure **5/5c** is characterized by an energy barrier of 159 kJ/mol. Ion **5c** is the starting point of the successive hydrogen shifts summarized in Scheme 4 which lead to structure **6a** encountered above.

Energies of the cyclic structures **5c**, **13**, and **14**, relative to NO$^+$ + ethylene, are equal to 2, −91, and 63 kJ/mol, respectively. Despite the noticeable stability of the intermediate **13**, the barriers separating each species are considerable, the highest (transition structure **5c/13**) being 208 kJ/mol above NO$^+$ + ethylene. As illustrated in Figure 4, the overall multistep process **5 → 5c → 13 → 14 → 6a** is disfavored with respect to the direct 1,3-hydrogen transfer **5 → 6a** mentioned above (see also Figure 3).

Structure **5** may also give rise to ions CH$_2$=CH–N=OH$^+$ (**7**) and CH$_3$–C≡N$^+$–OH (**8**) as depicted in Scheme 5. Direct formation of the latter by a hydrogen migration from the CH group of **5** to the oxygen atom needs a very large critical energy. On the other hand, a seemingly easier route is provided by the three-step process **5 → 7s → 7a → 8**, which implies first a 1,4-hydrogen migration, followed by rotation, and further by a 1,2-hydrogen shift. Structure **7a** may support several additional isomerization reactions. One possible route involves a 1,3-hydrogen migration of the hydrogen of a CH group to the oxygen in order to produce ion **10**. We were however not able to locate a transition structure for this reaction, which, in fact, appears to prefer to follow the two-step process **7a → 8 → 10**.

Gas-Phase Nitrosation of Ethylene

J. Phys. Chem. A, Vol. 112, No. 24, 2008 **5423**
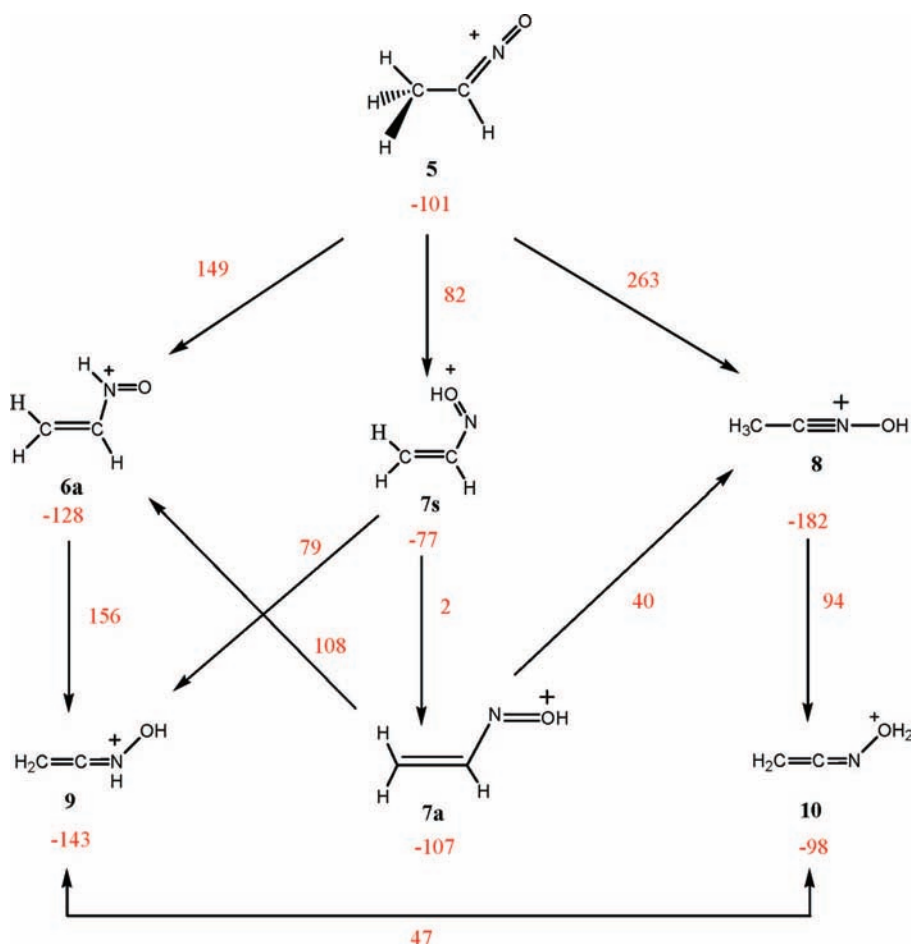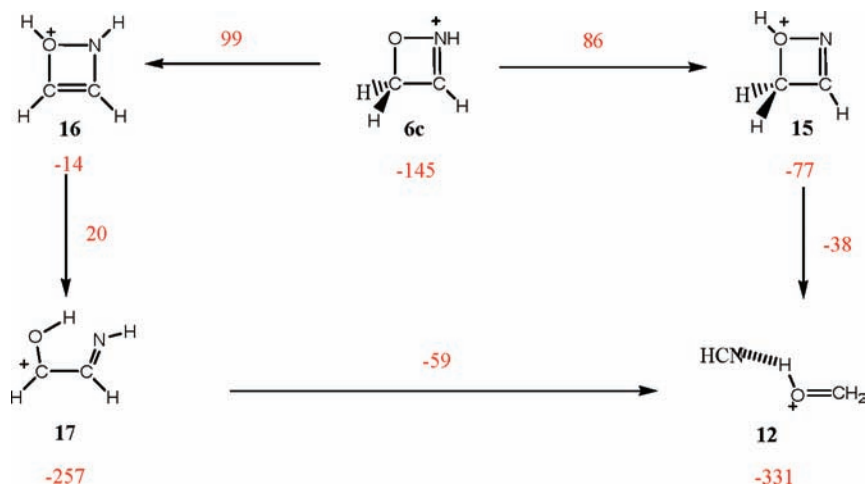
SCHEME 5

SCHEME 6

The global isomerization pathway presented in Scheme 5 also includes ion **6a**, which is connected to either ions **7a** or **9** by a 1,2-hydrogen migration from the nitrogen to the oxygen atoms or by a 1,3-hydrogen migration from the CH group to the oxygen atom. Both processes exhibit large critical energies since the corresponding transition structures **6a/7a** and **6a/9** are found 108 and 156 kJ/mol above NO$^+$ + ethylene, respectively.

Structure **9** can be more easily produced by isomerization of **7a** or **7s** by a 1,2-hydrogen shift from the CH group to the nitrogen atom. The corresponding transition structure **7s/9** is found 79 kJ/mol above NO$^+$ + ethylene. Finally, isomerization between structures **9** and **10** has been investigated. The easier

pathway for this rearrangement appears to be a direct 1,2-H shift **9** → **10** process rather than the passages through the chain of structures **5**–**8**. Figure 5 summarizes the 298 K enthalpy diagram corresponding to the isomerization routes of structure **5**.

Finally, we investigated the possibilities of isomerism from the cyclic structure **6c** whose formation from **1**–**3** has been evoked in Scheme 3. As described in Scheme 6, two 1,2-hydrogen shifts toward the oxygen atom lead to structure **15** or **16**, which are clearly less stable than their precursor **6c**. By contrast, both structures may evolve toward the very stable species **12** and **17**. Accordingly, ring opening of ion **15** readily
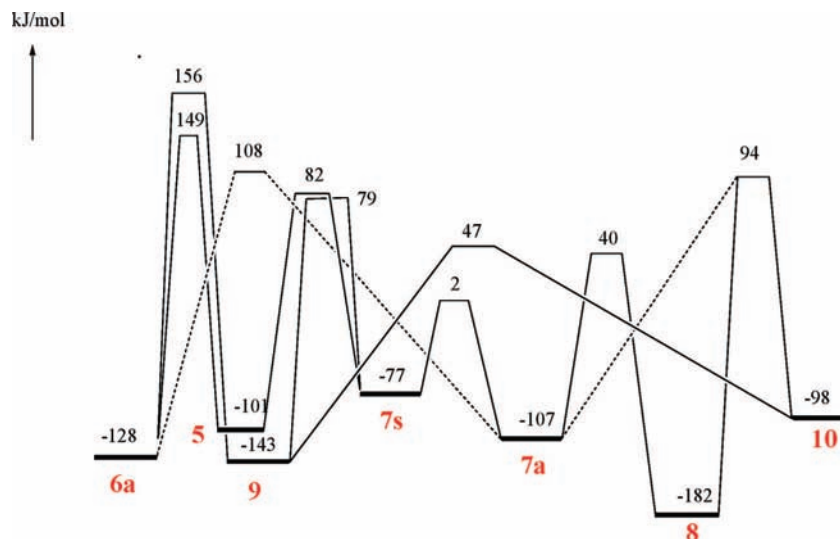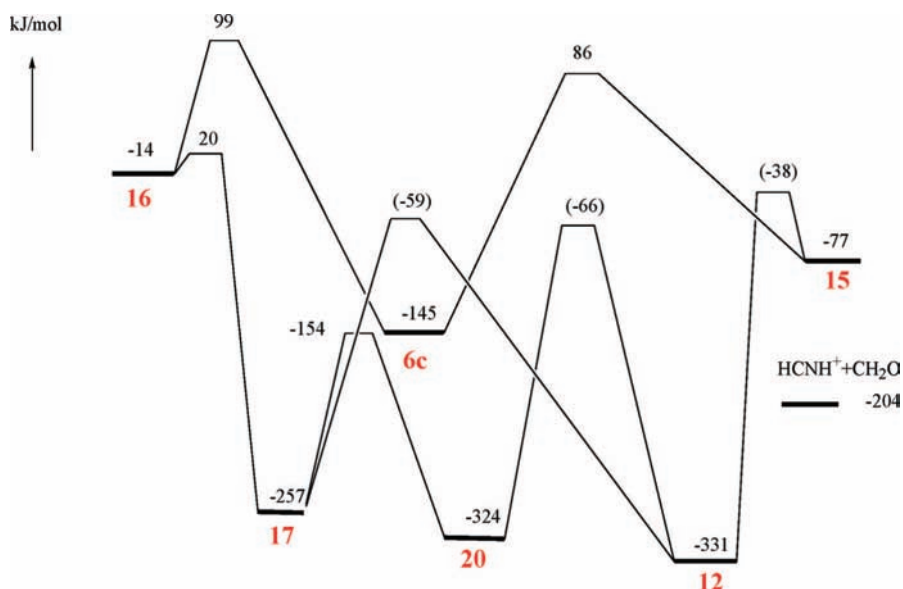
Figure 2. G3B3 (G2) 298 K enthalpy diagram for NO^+/C_2H_4 adducts **1−3** isomerization and ring opening to **4** and **11**.

Figure 3. G3B3 (G2) 298 K enthalpy diagram for isomerization of **1′** and **3** into **5** and **6**.

Figure 4. G3B3 (G2) 298 K enthalpy diagram for isomerization of **5** into **6a** via **5c**, **13**, and **14**.

converges in the direction of the ion-neutral complex **12**. Similarly, ring opening of ion **16** leads to the oxonium ion **17**. Let us note that besides structure **12**, another ion-neutral complex can be formed from interaction between $HCNH^+$ and CH_2O, in which the hydrogen attached to the cation carbon points toward the oxygen of formaldehyde. This structure, denoted as **12′**, is characterized by conservation of the two $HCNH^+$ and CH_2O substructures, in which the proton responsible of the hydrogen bond $CH_2O\cdots HCNH^+$ remains on the

carbon atom, in agreement with the larger proton affinity of HNC (772.3 kJ/mol)[2] with respect to CH_2O (712.9 kJ/mol).[2]

In order to interpret the experimental data concerning stable $(C_2H_4NO)^+$ species, which will be presented in the next paragraph, it is necessary to know not only the isomerization barriers separating the investigated ions from each other but also their dissociation limits. The energy levels corresponding to most of the possible dissociation products have thus been calculated, and the results are given in Table S2 of the Supporting Information. The first set of fragments presented in Table S2 (Supporting Information) involves the ethylene and NO moieties, which are produced from **1−3** by simple bond cleavage. Loss of a hydrogen atom may occur from all the considered structures and leads to a variety of $(C_2H_3NO)^{\cdot+}$ radical cations. Among the latter, one of the most stable forms is $CH_2=CHNO^{\cdot+}$, which is produced by simple bond cleavage from **1**, **5**, **6**, and **7**. Methyl cation formation is generally more favorable than methyl radical loss from $(C_2H_4NO)^+$ cations. A thorough examination of the various HCNO isomers has been done at the G2 level of theory by Bacskay and Shapley.[23] The global minimum of the singlet energy surface corresponds to isocyanic acid HNCO, followed by cyanic acid HOCN (relative energy of 106.3 kJ/mol at 0 K by G2 method), fulminic acid HCNO (293.3 kJ/mol), and isofulminic acid HONC (350.0 kJ/mol). Comparable relative energies are obtained here using the G2 level. It is noteworthy that the same order of stability is also found for the corresponding radical cations (Table S2, Supporting Information). The energy level of the products CH_3^+ + CHNO and $CHNO^{\cdot+}$ + $CH_3^{\cdot}$ are however different by ca. 200 kJ/mol. Finally, products involving neutral or protonated CH_2O and hydrogen cyanide are also presented in Table S2 (Supporting Information).

In summary, it is clear from the main results of the present calculations shown in Figures 2–6 that a number of $(C_2H_4NO)^+$ structures are protected against isomerization and dissociation by large energy barriers. Experimental characterization of various $(C_2H_4NO)^+$ species is thus possible if efficient collisional cooling is associated with formation of these ions as now presented.

Gas-Phase Nitrosation of Ethylene

J. Phys. Chem. A, Vol. 112, No. 24, 2008 **5425**

Figure 5. G3B3 298 K enthalpy diagram for **5**−**10** isomerization processes.

Figure 6. G3B3 (G2) 298 K enthalpy diagram for isomerization reactions of the cyclic ion **6c**.

Experimental Results

$C_2H_4 \cdot NO^+$ Ion 1. Direct condensation of NO^+ with ethylene in selected ion flow tube experiments at 298 K under a helium pressure of 0.46 Torr occurs at a rate lower than 10^{-3} the collision rate.[15] No reaction was observed by Hunt and Harvey[11a] when introducing ethylene in the nitric oxide plasma formed at 1 Torr in a chemical ionization source. We recently observed that a gas-phase nitrosation is seemingly possible from ion/molecule reaction using *tert*-butyl nitrite as reagent.[8] Therefore, we attempted to form the ethylene·NO^+ adduct by reaction between *tert*-butyl nitrite and the ethyl cation. Unfortunately, as expected from the relative proton affinities of ethylene and *tert*-butyl nitrite, it was 680 and 861 kJ/mol, respectively,[2] only the proton transfer reaction was observed.

We finally obtained a positive result when considering the ligand-exchange reaction (eq 1) in the quadrupole collision cell of the hybrid tandem mass spectrometer

$$H_2O \cdot NO^+ + C_2H_4 \rightarrow H_2O + C_2H_4 \cdot NO^+ \qquad (1)$$

The most stable form of protonated nitrous acid (HONO) unambiguously corresponds to protonation of the central

oxygen.[22,23] The equilibrium geometry of this ion corresponds to a complex between water and NO^+ ($H_2O \cdot NO$)$^+$. The next lower lying isomer $HONOH^+$ is ca. 150 kJ/mol higher in energy.[24] In our experiments, the $H_2O \cdot NO^+$ cations (*m/z* 48) are prepared by ionization of a mixture of nitric oxide ($NO^\bullet$) and water under chemical ionization conditions (source pressure ca. 1 Torr). The so-produced *m/z* 48 ions are then mass selected, decelerated to ca. 5 eV laboratory kinetic energy to maximize associative ion/molecule reaction yields, and then introduced in the quadrupole cell pressurized with ethylene. All the ions produced in the quadrupole cell are reaccelerated to 8 keV and mass analyzed by scanning the field of the second magnetic sector (see Experimental Section); the resulting mass spectrum is presented in Figure 7a. Besides the major signal associated with the mass-selected *m/z* 48 cations, this mass spectrum features a peak at *m/z* 58 corresponding to the expected NO^+ transfer from the mass-selected cations toward neutral ethylene and a peak at *m/z* 30 (NO^+) originating from dissociation of the nitroso ions.

The NO^+ binding energy of water is equal to about 78 kJ/mol,[6,21] and as established from the G2 and G3B3 calculations presented above, a similar quantity of 65 kJ/mol is obtained
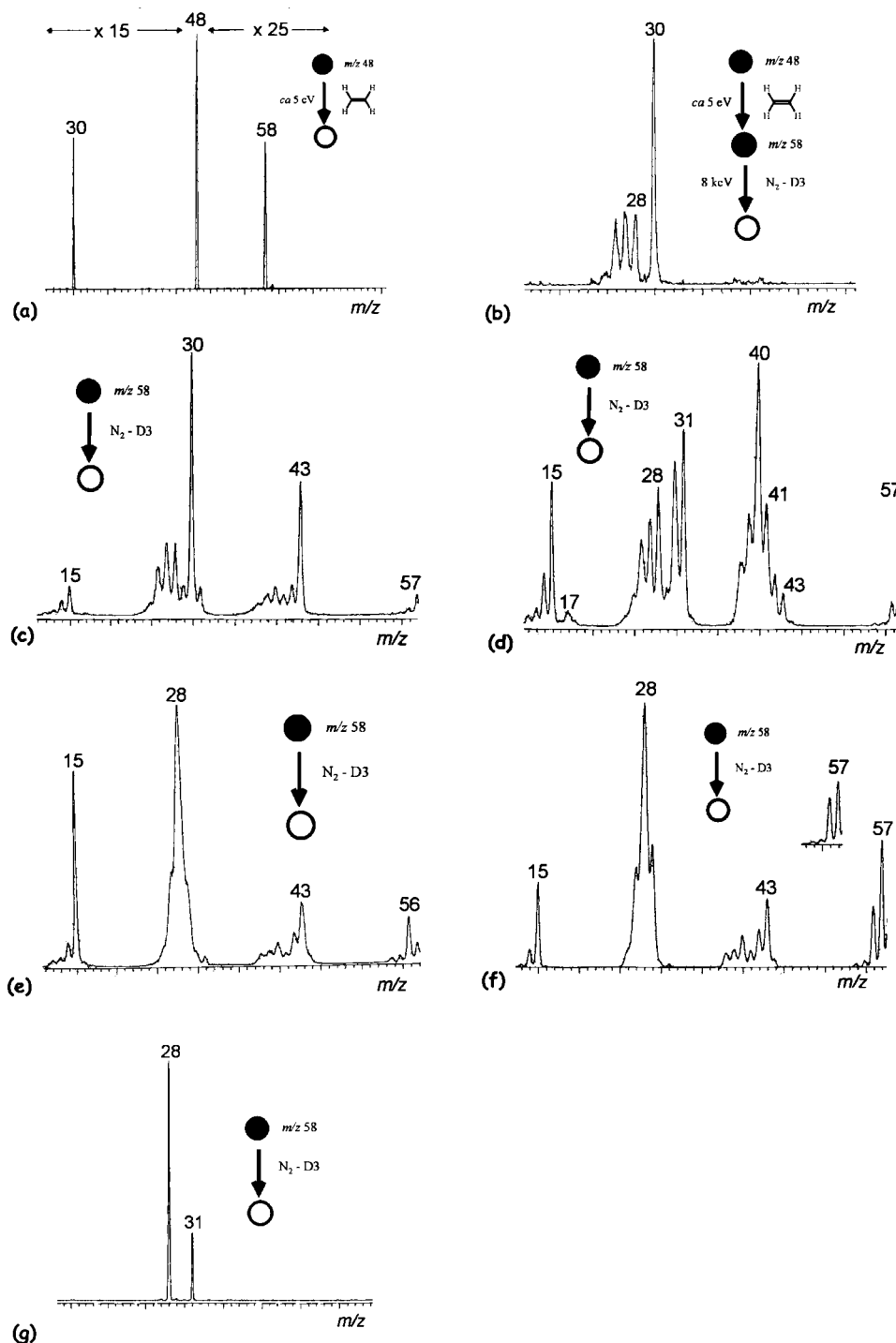
Figure 7. Collisional activation mass spectra of $C_2H_4NO^+$ ions. The terminology used to schematize the ion−molecule interactions is that introduced by Schwartz et al.:[25] a filled circle represents a fixed (or selected) mass and an open circle a variable (or scanned) mass, whereas the neutral reagent that causes the mass transition is shown between the circles (ref 25).

SCHEME 7
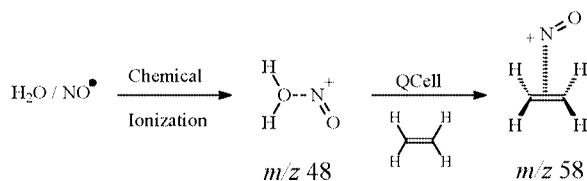
for ethylene if the most stable adduct **1** is considered. Obviously this quantity is reduced to ca. 13 and 28 kJ/mol if structures **2** and **3** are actually formed. Considering these data, reaction 1 is calculated to be endothermic by 13, 65, and 50 kJ mol^{-1} for

production of **1**, **2**, and **3**, respectively. Observation of a slightly endothermic process in our experiments is not unexpected because of the absence of a thermalization step before the associative interaction in the quadrupole cell. However, as far as the NO^+ transfer process is concerned, it has recently been observed that exchange reactions amounting to endothermicity as high as 40 kJ/mol are not detected.[21] As a consequence, it is expected that under our experimental conditions, only structure **1** is produced by reaction 1 (Scheme 7).

The structure of the *m/z* 58 cation **1** can be characterized by performing a subsequent collisional activation experiment. The

Gas-Phase Nitrosation of Ethylene

J. Phys. Chem. A, Vol. 112, No. 24, 2008 **5427**

SCHEME 8
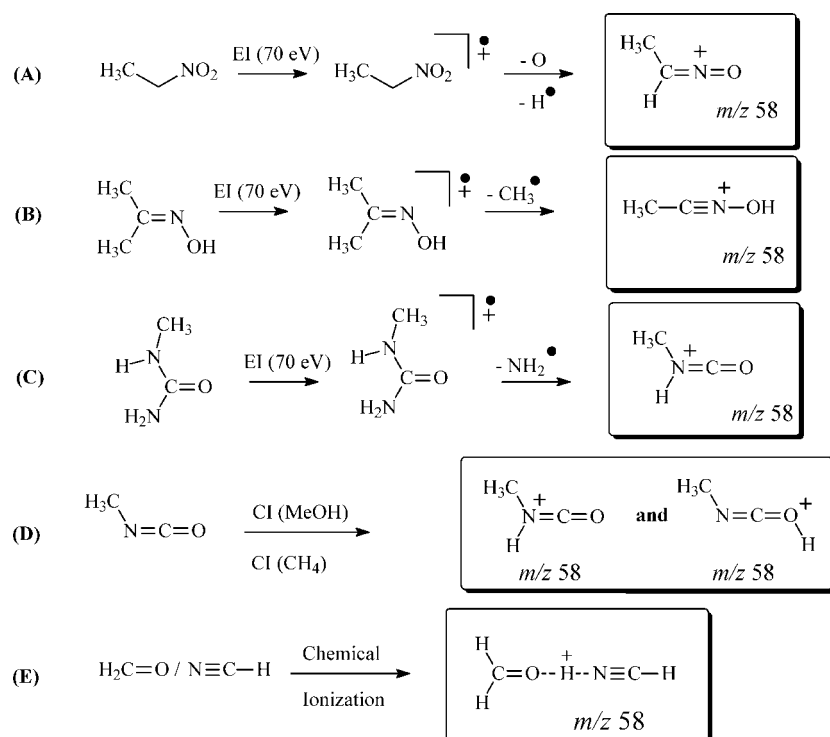
recorded CA mass spectrum, shown in Figure 7b, essentially exhibits signal at m/z 30 (NO^+) and m/z 28, 27, and 26 ($C_2H_4^{\bullet+}$, $C_2H_3^+$, and $C_2H_2^{\bullet+}$). The presence of those fragment ions is totally in keeping with a structure consisting of an ion-neutral complex binding the two moieties NO^+ and C_2H_4. Moreover, the peak intensities in Figure 7b are in qualitative agreement with the calculated energy levels of the two sets of products since $NO^+ + C_2H_4$ is situated 126 kJ/mol below $C_2H_4^{\bullet+} + NO$.

CH_3CHNO^+ Ion 5. The electron ionization mass spectrum of nitroethane shows a small signal at m/z 58 (about 1% of the m/z 29 base peak). The corresponding ions possess the C_2H_4NO composition and are likely to be $CH_3(H)CNO^+$ cations (Scheme 8A). Indeed, after collisional activation (Figure 7c), those cations competitively expel a hydrogen atom (m/z 57, $CH_2CHNO^{\bullet+}$), a methyl radical (m/z 43, $H-C≡N^+-O^{\bullet}$), C_2H_4 (m/z 30, NO^+), and HCNO (m/z 15, CH_3^+).

CH_3CNOH^+ Ion 8. Ionized acetoxime eliminates a methyl radical (Scheme 8B), and this decomposition is expected to produce $CH_3-C≡N^+-OH$ cation (**8**). The CA spectrum of the corresponding m/z 58 ions (Figure 7d) features sizable signals at $m/z = 57$, 31, and 15, which indicate different facile losses of H, C_2H_3, and CNOH, in agreement with the expected structure. To complement this attribution, we note small but significant peaks at m/z 43 ($CH_3^{\bullet}$ loss), 41 ($HO^{\bullet}$ loss), and 17 (HO^+ cations). The base peak at m/z 40, corresponding to $C_2H_2N^+$ cations, is also observed without collision gas and therefore arises from decomposition of metastable ions in an unimolecular process. A possible reaction is **8 → 10**, which in turn can eliminate a water molecule to give CH_2CN^+ (see Scheme 5).

Ions CH_3NHCO^+ (18) and CH_3NCOH^+ (19). Note that **5** and **8** are two protonated forms of methylcyanide oxide CH_3CNO. By comparison, protonation of methyl isocyanate CH_3NCO gives rise to CH_3NHCO^+ **18** and CH_3NCOH^+ **19** structures, which will be examined in this section.

Dissociative ionization of *N*-methylurea mainly leads to loss of a NH_2 radical and production of m/z 58 cations as exemplified in Scheme 8C. Again the recorded CA spectrum (Figure 7e) is characteristic of the expected structure, namely, N-protonated methyl isocyanate, $CH_3-N^+(H)=C=O$. Actually, the CA spectrum shows intense signals at m/z 43 (loss of $CH_3^{\bullet}$), 28 (ionized carbon monoxide), and 15 (methyl cation).

Direct protonation of methyl isocyanate was also realized under chemical ionization conditions using methanol as the CI gas (Scheme 8D). The recorded CA spectrum (Figure 7f) is similar to the CA spectrum of the m/z 58 cations prepared starting from methylurea, except for the hydrogen-atom loss being more pronounced in the case of the CI-generated cations. As an explanation we proposed that under CI conditions protonation of methyl isocyanate readily occurs either at the nitrogen atom or at the oxygen atom site, respectively, yielding $CH_3-N^+(H)=C=O$ and $CH_3-N=C=O^+H$ cations (Scheme 8D). The latter species is more prone to hydrogen-atom loss since it is 43 kJ/mol less stable than the former (298 K enthalpies difference at the G2 level and more intense m/z 57 signal in the corresponding CA spectrum Figure 7f). Both protonation reactions are calculated to be competitive under CI conditions with methane since the respective proton affinities (PA) are calculated, at the B3LYP/6-311++G(d,p) + ZPE level of theory, to amount to 754 and 714 kJ/mol at the nitrogen and oxygen atoms, respectively. Both sites are likely to be protonated by CH_5^+ [CI(methane)] as the PA(methane) is only 551 kJ/mol,[2] The inset in Figure 7f represents the m/z 56−57 signals from the CA spectrum of the m/z 58 cations prepared under CI methanol conditions. Under such softer conditions (with PA(methanol) = 761 kJ/mol[2]), competition between protonations at the nitrogen and oxygen sites is limited and we observed in the corresponding CA spectrum (inset in Figure 7f) a significant decrease of the intensity of the m/z 57 signal associated with the O-protonated species.

Ions $CH_2OH \cdot NCH^+$ (12) and $CH_2O \cdot HCNH^+$ (12'). Finally, one more isomeric ion is prepared by ionization under CI conditions of a mixture of hydrogen cyanide, HCN, and formaldehyde, $CH_2=O$ (Scheme 8E). The obtained m/z 58

cations are immediately identified as a proton bond dimer between HCN and $CH_2=O$ since the CA spectrum (Figure 7g) only features two signals corresponding to protonated hydrogen cyanide (*m/z* 28) and protonated formaldehyde (*m/z* 31).

Concluding Remarks

The present combined experimental and theoretical study includes an extended exploration of the $C_2H_4NO^+$ landscape with emphasis on the entrance by the ethylene plus NO^+ channel. Nineteen stable structures and a large set of their possible interconnections have been theoretically investigated at the G2 and G3B3 levels. This investigation provides us with a better understanding of the particularly rich chemistry of this ionized system. For example, NO^+ insertion and skeletal rearrangements evidenced in previous experimental works can be interpreted in light of reaction profiles illustrated by Schemes 2–6 and Figures 2–6.

Several structures predicted to be stable by the computation have been characterized *for the first time* by collisional activation in a six-sector mass spectrometer. The most stable complex formed between ethylene and NO^+ is a π complex (structure **1**), which can be produced in the gas phase by a transnitrosation process involving as reactant a complex between water and NO^+ $(H_2O \cdot NO)^+$ and the ethylene molecule. The stabilization energy of complex **1** is about 65 kJ/mol with respect to its separated components (G2 and G3B3 298 K enthalpy differences). Five other ionic structures were also identified including CH_3CHNO^+ (**5**), CH_3CNOH^+ (**8**), CH_3NHCO^+ (**18**), CH_3NCOH^+ (**19**), and an ion-neutral complex $CH_2O \cdots HCNH^+$ (**12**). It is noteworthy that the latter are among the $C_2H_4NO^+$ species whose high stability is established in the present work by calculations, most of them being situated ∼300 kJ/mol below structure **1**.

Supporting Information Available: Total and relative energies. This material is available free of charge via the Internet at http://pubs.acs.org.

References and Notes

(1) (a) A complete issue of *Chemical Reviews* has been devoted recently to nitric oxide chemistry: *Chem. Rev.* **2002**, *102*, 4. (b) See also: Grassian, V. H. *J. Phys. Chem. A* **2002**, *106*, 860–877.

(2) Lias, S.; Bartmess, J. E.; Liebman, J. F.; Holmes, J. L.; Levin, R. D.; Mallard, W. G. NIST Chemistry WebBook, Standard Reference Database; 1998, Vol. 69, http://webbook.nist.gov

(3) (a) Borodkin, G. I.; Shubin, V. G. *Russ. Chem. Rev.* **2001**, *70*, 211–230. (b) Zyk, N. V.; Nesterov, E. E.; Khlobystov, A. N.; Zefirov, N. S. *J. Org. Chem.* **1999**, *64*, 7121–7128.

(4) Reents, W. D.; Freiser, B. S. *J. Am. Chem. Soc.* **1980**, *102*, 271–276.

(5) Reents, W. D.; Freiser, B. S. *J. Am. Chem. Soc.* **1981**, *103*, 2791–2797.

(6) Cacace, F.; de Petris, G.; Pepi, F. *Proc. Natl. Acad. Sci. U.S.A.* **1997**, *94*, 3507–3512.

(7) Gwaltney, S. R.; Rosokha, S. V.; Head-Gordon, M.; Kochi, J. K. *J. Am. Chem. Soc.* **2003**, *125*, 3273–3283.

(8) Dechamp, N.; Gerbaux, P.; Flammang, R.; Bouchoux, G.; Nam, P. C.; Nguyen, M. T. *Int. J. Mass Spectrom.* **2004**, *232*, 31–40.

(9) Chiavarino, B.; Crestoni, M. E.; Fornarini, S.; Lemaire, J.; Maitre, P.; MacAleese, P *J. Am. Chem. Soc.* **2006**, *128*, 12553–12561.

(10) Robinet, J.; Baciu, C.; Cho, M. E.; Gauld, J. W *J. Phys. Chem. A* **2007**, *111*, 1981–1989.

(11) (a) Hunt, D. F.; Harvey, T. M. *Anal. Chem.* **1975**, *47*, 2136–2141. (b) Harrison, A. G. *Chemical Ionisation Mass Spectrometry*, 2nd ed.; CRC Press: Boca Raton, FL, 1992.

(12) Spanel, P.; Smith, D. *Int. J. Mass Spectrom.* **1998**, *181*, 1–10.

(13) Midey, A. J.; Williams, S.; Viggiano, A. A. *J. Phys. Chem. A* **2001**, *105*, 1574–1578.

(14) Diskin, A.; Wang, A.; Smith, D.; Spanel, P. *Int. J. Mass Spectrom.* **2002**, *218*, 87–101.

(15) Wilson, P. F.; Freeman, C. G.; McEwan, M. J. *Int. J. Mass Spectrom.* **2003**, *229*, 143–149.

(16) Raghavachari, K.; Reents, W. D.; Haddon, R. C. *J. Comput. Chem.* **1986**, *7*, 265–273.

(17) Bateman, R. H.; Brown, J.; Lefevere, M.; Flammang, R.; Van Haverbeke, Y. *Int. J. Mass Spectrom. Ion Processes* **1992**, *115*, 205.

(18) Flammang, R.; Van Haverbeke, Y.; Braybrook, C.; Brown, J. *Rapid Commun. Mass Spectrom.* **1995**, *9*, 795.

(19) Frisch, M. J. et al. *Gaussian 03*, Revision B.04; Gaussian, Inc.: Pittsburgh, PA, 2003.

(20) Nicolaides, N.; Rauk, A.; Glukhovtsev, M. N.; Radom, L. *J. Phys. Chem.* **1996**, *100*, 17460.

(21) Gerbaux, P.; Wantier, P.; Flammang, R. *J. Am. Soc. Mass. Spectrom.* **2003**, *15*, 344.

(22) Nguyen, M. T.; Hegarty, A. F. *J. Chem. Soc., Perkin Trans.* **1984**, *2*, 2037.

(23) Shapley, W. A.; Bacskay, G. B. *J. Phys. Chem. A* **1999**, *103*, 6624.

(24) Francisco, J. S. *J. Chem. Phys.* **2001**, *115*, 2117.

(25) Schwartz, J. C.; Wade, A. P.; Enke, C. G.; Cooks, R. G *Anal. Chem.* **1990**, *62*, 1809.

JP8011238